The Astrophysical Journal, 639:L21–L24, 2006 March 1

PROBING POST-NEWTONIAN PHYSICS NEAR THE GALACTIC BLACK HOLE WITH STELLAR REDSHIFT MEASUREMENTS

Shay Zucker,[1] Tal Alexander,[1,2] Stefan Gillessen,[3] Frank Eisenhauer,[3] and Reinhard Genzel[3]
Received 2005 August 29; accepted 2006 January 18; published 2006 February 6

ABSTRACT

Stars very close to the massive black hole (MBH) in the center of the Galaxy allow us to probe post-Newtonian (PN) physics in a yet unexplored regime of celestial mechanics. Recent advances in infrared spectroscopy enable us to take precise measurements of stellar redshift curves and thereby detect $\mathcal{O}(\beta^2)$ PN effects (gravitational redshift in the MBH's potential and the transverse Doppler shift). We use simulations to show that these effects can be decisively detected with existing instruments after ~10 years of observations. We find that neglecting these effects leads to statistically significant systematic errors in the derived MBH mass and distance.

Subject headings: black hole physics — Galaxy: center — gravitation — infrared: stars — relativity — techniques: radial velocities

1. INTRODUCTION

General relativity (GR) is the least tested theory of the four fundamental forces of nature. The $m \sim (3\text{–}4) \times 10^6\ M_\odot$ massive black hole (MBH) in the Galactic center (GC) and the stars around it (Eisenhauer et al. 2005; Ghez et al. 2005) provide us with a unique laboratory for detecting post-Newtonian (PN) effects and for probing GR (for a review, see Alexander 2005). Astrometric and spectroscopic monitoring of stars orbiting the MBH allow us to derive their orbital elements. The stars are observed at periapse distances as small as $r_p \lesssim 10^3 r_s$ ($r_s \equiv 2Gm/c^2$) with velocities as high as $\beta_p \sim \text{few} \times 0.01$ ($\beta \equiv v/c$). The highest relativistic parameter at periapse observed to date, $\Upsilon(r_p) \equiv r_s/r_p \gtrsim 1.5 \times 10^{-3}$, is a few times higher than that on the surface of a white dwarf (e.g., $\Upsilon = 5 \times 10^{-4}$ on Sirius B*, one of the most relativistic white dwarfs known; Adams 1925; Barstow et al. 2005). It could reach values as high as $\Upsilon \sim \text{few} \times 10^{-2}$ for stars with a periapse of a few times the tidal disruption radius (for yet smaller periapse, the orbit will no longer be geodetic due to the tidal interaction). For comparison, the high-precision confirmation of GR predictions in the Hulse-Taylor binary pulsar (PSR 1913+16) was for masses of ~1.4 $M_\odot$ with $\beta_p \sim 0.003$ and $\Upsilon \sim 5 \times 10^{-6}$ (Taylor & Weisberg 1989). Note that although some accretion processes occur at $\Upsilon \gtrsim \mathcal{O}(0.1)$, the complex physics of accretion and its many uncertainties severely limit the usefulness of accretion emission as a probe of GR.

The strong equivalence principle, and thus GR, predicts that PN effects should depend only on Υ, and not, for example, on the "compactness" of the central object (ratio of gravitational self-energy to rest-mass energy; Damour & Esposito-Farèse 1996). This is not necessarily the case for alternative theories of gravitation (see review by Will 2001). Thus, it is important to *empirically* explore PN effects in as wide a range of parameters and configurations as possible, without prior assumptions. Stellar orbits around the Galactic MBH enable us to probe an unexplored regime of celestial mechanics (Kramer et al. 2004) in terms of $\Upsilon(r_p)$, the mass scale of the relativistic object and its compactness.

[1] Faculty of Physics, Weizmann Institute of Science, P.O. Box 26, Rehovot 76100, Israel; shay.zucker@weizmann.ac.il.
[2] The William Z. and Eda Bess Novick career development chair.
[3] Max-Planck-Institut für extraterrestriche Physik, Postfach 1312, Garching D-85741, Germany.

At present, all the observed orbits are well modeled by Newtonian physics. With improved resolution, higher precision, and a longer baseline, deviations from Keplerian orbits may be detectable. In this Letter we examine the future detectability of leading-order (β^2) PN effects with *existing* instrumental capabilities. We show that such effects can be detected in the observed stellar redshift curves (note that the redshift is no longer equivalent to radial velocity in the PN regime). We also find that the omission of these effects from the orbital solutions can lead to statistically significant systematic errors in the derived mass and distance of the MBH.

The measurement of stellar proper motions in the inner arcsecond (0.04 pc) of the GC (Eckart & Genzel 1996; Ghez et al. 1998) preceded by more than a decade the measurement of stellar radial velocities (Ghez et al. 2003; Eisenhauer et al. 2003a). Thus, most theoretical studies of the detectability of PN orbital effects focused on proper-motion–related effects, such as the periapse shift (e.g., Rubilar & Eckart 2001; Weinberg et al. 2005). However, with the advent of adaptive optics–assisted IR imaging spectroscopy (e.g., VLT/SINFONI; Eisenhauer et al. 2003b), it is now the redshifts rather than the proper motions that provide the tightest constraints on deviations from Newtonian orbits. Stellar spectroscopy in the GC now allows us to determine the redshift, z, to within $\delta z \sim 25$ km s$^{-1}/c$, or $\delta\lambda/\lambda \sim 10^{-4}$ (Eisenhauer et al. 2005).

The observed redshift curve $z(t)$ can be expanded in terms of the three-dimensional source velocity $\beta(t')$, where t' and t are the light emission and arrival times, respectively,

$$z = \Delta\lambda/\lambda = B_0 + B_1\beta + B_2\beta^2 + \mathcal{O}(\beta^3). \quad (1)$$

As shown in § 2, two effects contribute to the β^2-term (Kopeikin & Ozernoy 1999), $B_2 = B_{2,\mathrm{D}} + B_{2,G}$: the special relativistic (SR) transverse Doppler effect, with $B_{2,\mathrm{D}} = \frac{1}{2}$, and the GR gravitational redshift, with $B_{2,G} = \frac{1}{2}$. The $\mathcal{O}(\beta^2)$ effects are detectable with existing instruments, since $(B_{2,\mathrm{D}} + B_{2,G})\beta_p^2 \sim 10^{-3} > \delta\lambda/\lambda \sim 10^{-4}$.

2. β^2 EFFECTS IN THE REDSHIFT

When $\Upsilon \ll 1$, the orbit is Keplerian to a good approximation, and the orbital energy equation is

$$\beta^2 \simeq r_s/r - r_s/2a, \quad (2)$$

where a is the orbital semimajor axis. For an eccentric orbit,

$r_p \ll a$, and so near periapse $\Upsilon \sim \beta^2$. Two effects contribute to the β^2-term of the redshift expansion (eq. [1]). One is the GR gravitational redshift,

$$z_G \equiv (1 - r_s/r)^{-1/2} - 1 \simeq r_s/2r, \quad (3)$$

which also contributes a constant to the zeroth-order term of the z-expansion, $z_G = r_s/4a + \frac{1}{2}\beta^2 = B_{0,G} + B_{2,G}\beta^2$ (eq. [2]). The second is the relativistic Doppler shift of a moving source seen by an observer at rest,

$$z_D \equiv (1 + \beta \cos \vartheta)\Big/\sqrt{1 - \beta^2} - 1 \simeq \beta \cos \vartheta + \beta^2/2, \quad (4)$$

where ϑ is the angle between the velocity vector and the line of sight. The Newtonian Doppler shift, $z_N \equiv \beta \cos \vartheta = B_1\beta$, is the first-order term in the z-expansion. The SR transverse Doppler effect, $z_T \equiv \beta^2/2 = B_{2,D}\beta^2$, contributes to the β^2-term in the z-expansion.

The light-travel time from the star to the observer changes with the orbital phase in an inclined orbit. We include this effect, known as the Rømer delay, by relating the observed redshift $z(t)$ to the actual velocity at emission $\beta\{t - [R_0 - r(t') \cos \psi(t')]/c\}$, where ψ is the angle between $\boldsymbol{r}$ and the line of sight and R_0 is the distance to the MBH. This must be done because the Rømer delay, if unaccounted for, also contributes to the β^2-term (e.g., Alexander 2005).

The gravitational redshift and the transverse Doppler shift affect only the measured redshifts but not the astrometric proper motions. These are treated here as Newtonian, since astrometric PN effects are below the current astrometric precision. Figure 1 shows the $\mathcal{O}(\beta^2)$ effects that are predicted for the star S2, based on the orbital elements derived for it from a Newtonian fit to the data (Eisenhauer et al. 2005). As expected, the PN effects near periapse are a few percent of the total measured redshift, since for $z_T + z_G \ll 1$,

$$(z_T + z_G)/z \sim \beta_p^2/\beta_p \sim \beta_p. \quad (5)$$

Brumberg et al. (1975) studied the detectability of the gravitational redshift and transverse Doppler shift effects in binary pulsar timing data. They show that radial velocity data alone are not enough for detecting the effects, since to leading order they can be absorbed in a purely Newtonian solution by very small modifications of the orbital elements K (radial velocity amplitude), ω (argument of the periapse), and V_0 (the line-of-sight center-of-mass velocity). To break the degeneracy, they suggest using the GR periapse shift ($\dot{\omega} \neq 0$). This is feasible for a binary pulsar, where the orbital period P is very short and the timing is extremely accurate, but not for the orbits around the Galactic MBH. In this context there are two possibilities to break the degeneracy. One is to use the astrometric data, which can constrain both ω and K. Another is to use the fact that the stars all orbit a common center of mass and share the same V_0. Thus, a combined astrometric and radial velocity orbital solution for all the stars can break the degeneracy and reveal the $\mathcal{O}(\beta^2)$ effects.

Newtonian orbital elements and their errors are usually obtained by a χ^2 fit of Newtonian orbits to the data. Following the phenomenological approach of Kopeikin & Ozernoy (1999), we extend this procedure by introducing a new parameter, X_2, to quantify the strength of the $\mathcal{O}(\beta^2)$ effects,

$$z = B_0 + B_1\beta + X_2\beta^2, \quad (6)$$

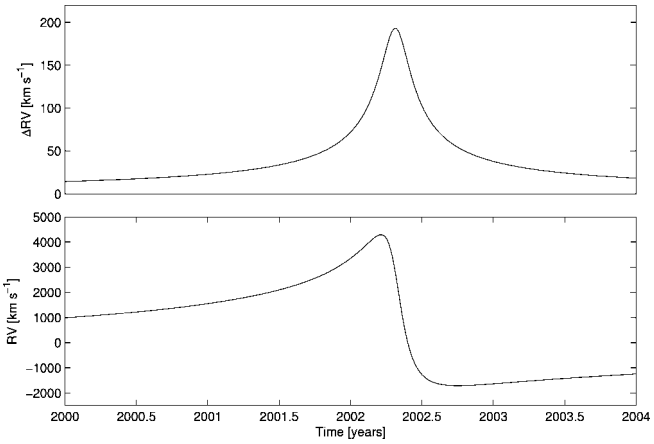

FIG. 1.—*Bottom*: Full relativistic radial velocity curve of S2 near periapse. *Top*: Contribution of the PN β^2 effects of the gravitational redshift and transverse Doppler shift to the total.

where the PN terms in B_0 are degenerate with the velocity of the local standard of rest relative to the GC. The $\mathcal{O}(\beta^2)$ effects include both the SR Doppler effect and the GR gravitational redshift, which cannot be separated empirically at the current level of measurement precision. The PN contribution in the Doppler term can be formally parameterized as

$$z_D(X_D) = (1 + \beta \cos \vartheta)\Big/\sqrt{1 - X_D\beta^2} - 1. \quad (7)$$

For SR, $X_D = 1$. The PN contribution in the GR gravitational redshift term can be parameterized as

$$z_G(X_G) = (1 - X_G r_s/r)^{-1/2} - 1. \quad (8)$$

For GR, $X_G = 1$. Therefore, the measured PN parameter is $X_2 = (X_D + X_G)/2$. In other relativity tests, where the potential difference is measured directly, it is customary to use $\alpha = X_G - 1$ (e.g., Will 1981), which translates to $\alpha = 2(X_2 - 1)$. In practice, we assume throughout that SR holds and that $X_D = 1$. For Newtonian physics, $X_2 = 0$, for PN SR physics without GR, $X_2 = \frac{1}{2}$, and for PN GR, $X_2 = 1$. Other values are also possible, in principle, and would indicate deviations from the predictions of these theories. If future data quality or candidate alternative theories warrant it, the fit procedure can be easily generalized to include multiple PN parameters.

We looked for evidence of PN effects in the published orbital data of the six stars S1, S2, S8, S12, S13, and S14 (Eisenhauer et al. 2005). We obtain a best-fit value of $X_2 = -4.9 \pm 2.9$, which appears to exclude PN GR at a 0.02 confidence level, PN SR physics at a 0.03 confidence level, and Newtonian physics at a 0.05 confidence level. The number of currently available redshift measurements is very small, and the astrometric data are not homogeneous. It is conceivable that these results are strongly influenced by systematic effects. Future observations will help us settle this question.

3. SIMULATIONS

We performed a suite of simulations to investigate the detectability of $\mathcal{O}(\beta^2)$ effects in the redshift data with existing instrumental capabilities and with realistic astrometric and spectroscopic precision. Since the relative strength of the PN effects scales with β_p (eq. [5]), stars that pass through deep (high-velocity) periapse during the monitoring period have the most impact on the detectability of the PN effects. This has

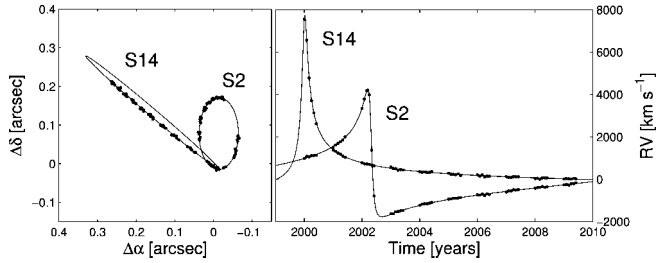

FIG. 2.—Simulated orbits of the stars S2 and S14. The "observed" astrometric data (*left*) and redshift data (*right*) are marked by points.

actually happened in the period 2000–2003 (Eisenhauer et al. 2005; Fig. 2) for the two stars S2 (with $P = 15.2$ yr, eccentricity $e = 0.88$, $r_p = 1500r_s$, $\beta_p = 0.02$) and S14 (with $P = 38$ yr, $e = 0.94$, $r_p = 1400r_s$, $\beta_p = 0.03$). Unfortunately, at that time, precise stellar spectroscopy of the inner GC was just becoming available, and only a few Doppler measurements of S2 were obtained (Ghez et al. 2003; Eisenhauer et al. 2003a).

To make the simulations realistic, we used the six orbits monitored and solved by Eisenhauer et al. (2005), and five additional stars that are currently being monitored and for which tentative orbital solutions exist. These five solutions are not yet reliable, but they can serve as a statistically representative sample, similar to the actual orbits that will be solved in the near future. Based on their periods (79, 204, 47, 64, and 800 yr) and corresponding eccentricities (0.470, 0.408, 0.848, 0.940, and 0.992), we synthesized mock orbits, M1–M5. M5 goes through deep periapse within the monitoring period.

We generated in total 11 synthetic orbits. The simulated data sets consisted of one observation per month (two astrometric coordinates and one redshift per star), for 6 consecutive months per year (the GC is observable only part of the year). The starting point was the year 2000, so the first 3 years already cover the periapse passage of S2 and S14 (Fig. 2). To each measurement, we added uncorrelated random Gaussian errors, with a standard deviation of 25 km s^{-1} for the radial velocities and 1.5 mas per coordinate for the astrometry, which are representative of the measurement errors for S2. The MBH's astrometric position and proper motion were assumed to be known, since frequent accretion flares can reveal the MBH's location (Genzel et al. 2003a; Ghez et al. 2004). These assumptions are somewhat optimistic since S2 is better measured than most stars and since the accurate localization of the MBH by the flares is still challenging. However, judging from the continuing improvement in data acquisition, it is not unreasonable to expect such data quality in the near future.

We generated synthetic data sets starting from 3 years and up to 20 years. We repeated the entire procedure twice, both with and without the PN GR effect (PN SR was included in both). We then applied the PN orbital fit procedure to the simulated data sets and recorded the best-fit values of X_2.

The upper panel of Figure 3 shows the derived values of X_2 for both PN SR and PN GR simulated orbits of the 11 stars (of which only S2, S14, and M5 go through deep periapse). The errors on X_2 clearly improve with longer monitoring. The two hypotheses can be decisively distinguished by the data at better than a 4 σ confidence level already after 10 years of monitoring (note that this implies the rejection of pure Newtonian orbits at an 8 σ confidence level). The lower panel translates the errors on X_2 into the expected detection significance for 1 (S2 only), 6 (published orbits, including S2 and S14), and all 11 stars. These confidence levels reflect the assumed measurement errors. The effect of a change in the assumed errors can be easily assessed by noting that a global scaling of all errors simply scales the confidence interval by the same factor.

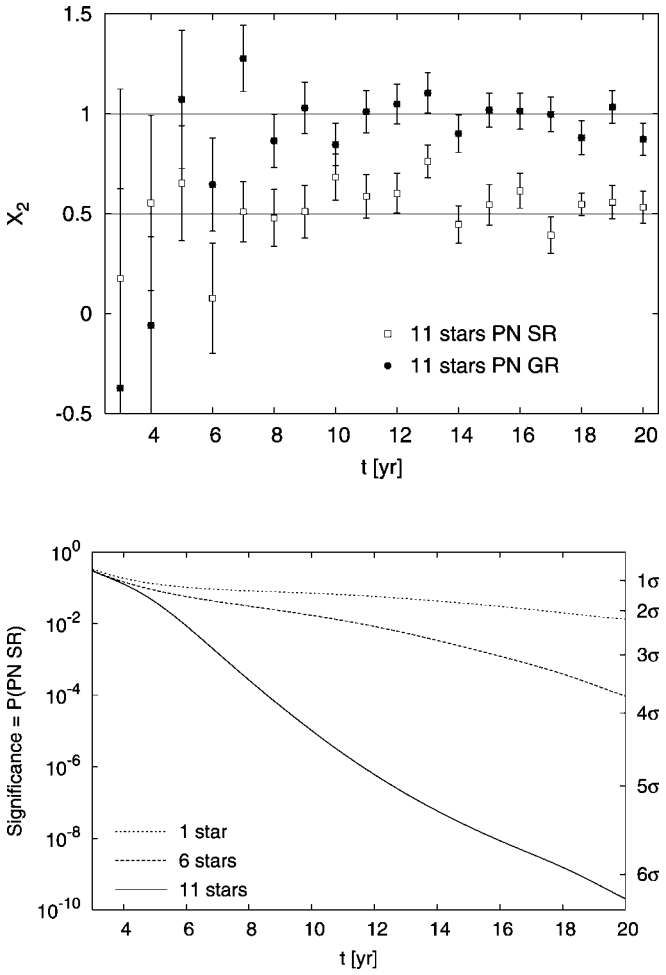

FIG. 3.—*Top*: 1 σ limits on the best-fit X_2 parameter [$X_2 = \frac{1}{2}$ for PN SR and $X_2 = 1$ for PN GR; in terms of Will's (1981) notation, $\alpha = 2(X_2 - 1)$]. *Bottom*: Mean significance of detection of the PN GR effects in the simulated data set with PN GR, as a function of monitoring time for 1, 6, and 11 stars, presented in terms of the rejection probability (*left axis*) and as standard deviations (*right axis*).

4. DISCUSSION

Stellar orbits around the Galactic MBH allow us to probe an unexplored regime of celestial mechanics in terms of the relativistic parameter at periapse, the mass scale of the relativistic object and its compactness (Kramer et al. 2004). We demonstrated that leading-order PN GR effects in the redshifts of stars orbiting the Galactic MBH can be decisively detected (at >4 σ confidence level, or <25% accuracy) in about a decade of astrometric and spectroscopic monitoring with existing instruments. Future observations of a larger number of stars and more deep periapse passages may well improve these results. It should be noted that GR gravitational redshift has already been confirmed with 6% accuracy on the surface of a white dwarf (Barstow et al. 2005), albeit at quite a different regime in terms of the mass scale and compactness.

Radial velocity data enable us to derive both the MBH mass, m, and distance to the GC, R_0, without prior assumptions (Salim & Gould 1999). If ignored, the PN effects can introduce systematic errors in the best-fit values of these parameters. For example, the omission of the gravitational redshift, transverse

Doppler and Rømer effects (usually ignored in current analyses) biases the best-fit values in our 11-star simulation from the input values of $m = 3.61 \times 10^6\ M_\odot$ and $R_0 = 7.62$ kpc to the derived values $m = (3.76 \pm 0.02) \times 10^6\ M_\odot$ and $R_0 = 7.73 \pm 0.02$ kpc. These constitute relative errors of 4% and 1.5% in the derived values of m and R_0, respectively, or $>5\ \sigma$ discrepancies. Such a mass discrepancy is of the same magnitude as the enclosed stellar mass within $\mathcal{O}(0.1$ pc) of the MBH (Genzel et al. 2003b). Thus, future attempts to detect dynamically the distributed dark mass on such scales (e.g., compact objects, faint stars), must take into account PN effects in the orbital solutions.

Another closely related PN effect is phase-dependent stellar flux variability. This is due to the combined effects of relativistic beaming and the Doppler shift. To leading order, beaming causes the bolometric flux to scale as $1 - 4\beta \cos \vartheta$ (Rybicki & Lightman 1979, eq. [4.97b]; Loeb & Gaudi 2003). However, since the infrared bands lie in the Rayleigh-Jeans part of typical S star spectra, the flux in the emitted spectral range that is observed after being Doppler-shifted scales as $1 + 3\beta \cos \vartheta$. Therefore, the total variability scales as $1 - \beta \cos \vartheta$, which translates to an expected variability near periapse of order $\beta_p \sim \mathcal{O}(0.01)$. Such variability, if detected by future instruments, will allow us to take an independent photometric measurement of the redshift curve.

We note that the effects of any dark distributed mass around the MBH on the redshift are likely to be small, but perhaps not completely negligible. The change in the redshift at periapse, $\delta z_{\rm dm}$, due to the retrograde periapse shift, $\delta\omega_{\rm dm}$, that is induced by the gravitational potential perturbation of the dark mass (see Alexander 2005) is of the order $\delta z_{\rm dm} \sim \mathcal{O}(|\delta\omega_{\rm dm}|\ \beta_p)$. This perturbation can be neglected as long as $|\delta\omega_{\rm dm}| \ll \beta_p \sim 0.01$. The periapse shift due to the hypothesized particle dark matter cusp is completely negligible (e.g., Gnedin & Primack 2004). The periapse shift in the orbit of S2 due to the observed luminous stellar mass (Genzel et al. 2003b) is only $|\delta\omega_{\rm dm}| \sim 3 \times 10^{-4}$. The possible shift due to an extreme case of mass segregation of stellar black holes (Alexander & Livio 2004) may be as high as $|\delta\omega_{\rm dm}| \sim 10^{-3}$.

The chances of detecting PN effects can be improved by optimizing the observing strategy. Generally, the observational program should focus on deep periapse passages and include as many stellar orbits as possible to better constrain the parameters and break the Newtonian/PN degeneracy. Our simulations were all based on the currently observed orbits and assumed optimal observing conditions. However, future observations will include additional orbits and be carried under varying observing conditions, which were not considered here. A comprehensive study of a range of orbital configurations, measurement errors, and observational resource allocation strategies remains to be done.

To summarize, we have shown that recent advances in infrared stellar spectroscopy enable us to decisively detect $\mathcal{O}(\beta^2)$ PN effects in the redshift curves with existing instruments after about a decade of observations.

We thank Re'em Sari for important comments. T. A. is supported by ISF grant 295/02-1, Minerva grant 8563, and a New Faculty grant by Sir H. Djangoly, CBE, of London, UK.

REFERENCES

Adams, W. S. 1925, Proc. Natl. Acad. Sci., 11, 382
Alexander, T. 2005, Phys. Rep., 419, 65
Alexander, T., & Livio, M. 2004, ApJ, 606, L21
Barstow, M. A., Bond, H. E., Holberg, J. B., Burleigh, M. R., Hubeny, I., & Koester, D. 2005, MNRAS, 362, 1134
Brumberg, V. A., Zel'dovich, Ya. B., Novikov, I. D., & Shakura, N. I. 1975, Soviet Astron. Lett., 1, 2
Damour, T., & Esposito-Farèse, G. 1996, Phys. Rev. D, 54, 1474
Eckart, A., & Genzel, R. 1996, Nature, 383, 415
Eisenhauer, F., Schödel, R., Genzel, R., Ott, T., Tecza, M., Abuter, R., Eckart, A., & Alexander, T. 2003a, ApJ, 597, L121
Eisenhauer, F., et al. 2003b, Proc. SPIE, 4841, 1548
———. 2005, ApJ, 628, 246
Genzel, R., Schödel, R., Ott, T., Eckart, A., Alexander, T., Lacombe, F., Rouan, D., & Aschenbach, B. 2003a, Nature, 425, 934
Genzel, R., et al. 2003b, ApJ, 594, 812
Ghez, A. M., Klein, B. L., Morris, M., & Becklin, E. E. 1998, ApJ, 509, 678
Ghez, A. M., Salim, S., Hornstein, S. D., Tanner, A., Lu, J. R., Morris, M., Becklin, E. E., & Duchêne, G. 2005, ApJ, 620, 744
Ghez, A. M., et al. 2003, ApJ, 586, L127
———. 2004, ApJ, 601, L159
Gnedin, O. Y., & Primack, J. R. 2004, Phys. Rev. Lett., 93, 061302
Kopeikin, S. M., & Ozernoy, L. M. 1999, ApJ, 523, 771
Kramer, M., Backer, D. C., Cordes, J. M., Lazio, T. J. W., Stappers, B. W., & Johnston, S. 2004, NewA Rev., 48, 993
Loeb, A., & Gaudi, B. S. 2003, ApJ, 588, L117
Rubilar, G. F., & Eckart, A. 2001, A&A, 374, 95
Rybicki, G. B., & Lightman, A. P. 1979, Radiative Processes in Astrophysics (New York: Wiley)
Salim, S., & Gould, A. 1999, ApJ, 523, 633
Taylor, J. H., & Weisberg, J. M. 1989, ApJ, 345, 434
Weinberg, N. N., Milosavljević, M., & Ghez, A. M. 2005, ApJ, 622, 878
Will, C. M. 1981, Theory and Experiment in Gravitational Physics (Cambridge: Cambridge Univ. Press)
———. 2001, Living Rev. Relativ., 4, 4